ESC European Society of Cardiology

Cardiovascular Research (2022) **118**, 489–502
doi:10.1093/cvr/cvab076

Pharmacological treatment with FGF21 strongly improves plasma cholesterol metabolism to reduce atherosclerosis

Cong Liu [1,2], Milena Schönke[1,2], Enchen Zhou [1,2], Zhuang Li[1,2], Sander Kooijman [1,2], Mariëtte R. Boon[1,2], Mikael Larsson [3], Kristina Wallenius [3], Niek Dekker [4], Louise Barlind[4], Xiao-Rong Peng[3], Yanan Wang[1,2,5], and Patrick C.N. Rensen [1,2,5]*

[1]Department of Medicine, Division of Endocrinology, Leiden University Medical Center, P.O. Box 9600, 2300 RC Leiden, The Netherlands; [2]Einthoven Laboratory for Experimental Vascular Medicine, Leiden University Medical Center, Leiden, The Netherlands; [3]Cardiovascular, Renal and Metabolism, AstraZeneca BioPharmaceutical R&D, Gothenburg, Sweden; [4]Discovery Sciences, AstraZeneca BioPharmaceutical R&D, Gothenburg, Sweden; and [5]Department of Endocrinology, First Affiliated Hospital of Xi'an Jiaotong University, Xi'an Jiaotong University, Xi'an, China

Received 19 December 2020; editorial decision 28 February 2021; accepted 4 March 2021; online publish-ahead-of-print 8 March 2021

Aims Fibroblast growth factor (FGF) 21, a key regulator of energy metabolism, is currently evaluated in humans for treatment of type 2 diabetes and non-alcoholic steatohepatitis. However, the effects of FGF21 on cardiovascular benefit, particularly on lipoprotein metabolism in relation to atherogenesis, remain elusive.

Methods and results Here, the role of FGF21 in lipoprotein metabolism in relation to atherosclerosis development was investigated by pharmacological administration of a half-life extended recombinant FGF21 protein to hypercholesterolaemic APOE*3-Leiden.CETP mice, a well-established model mimicking atherosclerosis initiation and development in humans. FGF21 reduced plasma total cholesterol, explained by a reduction in non-HDL-cholesterol. Mechanistically, FGF21 promoted brown adipose tissue (BAT) activation and white adipose tissue (WAT) browning, thereby enhancing the selective uptake of fatty acids from triglyceride-rich lipoproteins into BAT and into browned WAT, consequently accelerating the clearance of the cholesterol-enriched remnants by the liver. In addition, FGF21 reduced body fat, ameliorated glucose tolerance and markedly reduced hepatic steatosis, related to up-regulated hepatic expression of genes involved in fatty acid oxidation and increased hepatic VLDL-triglyceride secretion. Ultimately, FGF21 largely decreased atherosclerotic lesion area, which was mainly explained by the reduction in non-HDL-cholesterol as shown by linear regression analysis, decreased lesion severity, and increased atherosclerotic plaque stability index.

Conclusion FGF21 improves hypercholesterolaemia by accelerating triglyceride-rich lipoprotein turnover as a result of activating BAT and browning of WAT, thereby reducing atherosclerotic lesion severity and increasing atherosclerotic lesion stability index. We have thus provided additional support for the clinical use of FGF21 in the treatment of atherosclerotic cardiovascular disease.

* Corresponding author. Tel: +31-71-526-3078; fax: +31-71-524-8136, E-mail: P.C.N.Rensen@lumc.nl

Graphical Abstract

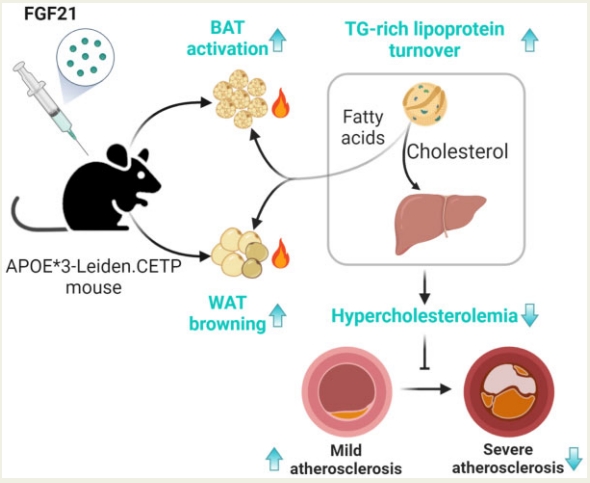

Keywords Adipose-liver axis • Brown adipose tissue • Atherosclerotic cardiovascular disease • Dyslipidaemia • Lipoprotein metabolism

1. Introduction

Atherosclerosis, which underlies life-threatening cardiovascular diseases, is driven by hypercholesterolaemia.[1] Apolipoprotein (Apo) B-containing cholesterol-rich lipoproteins enter the arterial intima to trigger or propagate a complex inflammatory cascade accompanied by cholesterol-laden foam cell accumulation, fatty streak formation, and subsequently the progressive development of atherosclerotic plaques.[1] Cholesterol homoeostasis in the circulation thus modulates the initiation and severity of atherosclerosis. The attenuation of hypercholesterolaemia potently reduces morbidity and mortality of atherosclerotic cardiovascular diseases as consistently observed in extensive clinical studies.[2] However, many at-risk patients either fail to reach their target cholesterol levels with current therapeutics such as statins or are intolerant to statins due to their adverse effects.[3] This leaves many patients with obvious residual risks, indicating that additional effective therapeutics including novel cholesterol-lowering agents are needed.

Fibroblast growth factor (FGF) 21, an endocrine hormone, has received increasing attention for its ability to regulate energy homoeostasis and counteract obesity-related disorders.[4,5] Physiologically, FGF21 is induced by a diverse range of stressors such as cold exposure, fasting/starvation, and ketogenic diet consumption, and in turn aids the adaptation to the stressor by increasing adaptive thermogenesis, lipolysis, ketogenesis, and fatty acid (FA) oxidation, respectively.[6–8] Moreover, patients with obesity,[9] type 2 diabetes,[10] and non-alcoholic fatty liver diseases[11] show higher serum FGF21 levels, demonstrating a compensatory FGF21 response in an attempt to overcome FGF21 resistance or maintain metabolic homoeostasis. FGF21 treatment has multiple therapeutic benefits for cardiometabolic disorders in rodents and humans, including alleviation of insulin resistance[5] and attenuation of non-alcoholic steatohepatitis.[12]

FGF21 exerts its metabolic actions through cell-surface receptors comprised of the conventional FGF receptor 1 in complex with β-klotho, which is abundantly expressed in fat tissue.[13] Despite adipose tissue being its primary target organ,[14] FGF21 also acts on the hypothalamus,[15] hindbrain,[16] and liver[8] to sustain metabolic homoeostasis. FGF21 was recently shown to directly and indirectly (via the sympathetic nervous system) act on adipose tissue to promote brown fat activation and white fat browning, thereby increasing energy expenditure and promoting weight loss.[17,18]

Studies on the role of FGF21 in atherosclerosis development are still scarce and mainly derived from genetic studies, showing that FGF21-deficiency in ApoE-knockout mice increases atherosclerosis.[19] Strikingly, FGF21 administration improves hypercholesterolaemia in obese non-human primates[20] and humans,[21] implying that beneficial effects of FGF21 on lipoprotein metabolism may attenuate atherosclerosis progression. Indeed, increased circulating FGF21 levels in atherosclerosis patients are proposed to be a compensatory mechanism to prevent vascular damage.[22] A single study has evaluated the pharmacological effect of FGF21 on atherosclerosis in FGF21 and ApoE double-knockout mice.[19] However, since ApoE is essential for mediating uptake of triglyceride (TG)-rich lipoprotein remnants by the liver, ApoE-knockout mice may not be the preferred model to study potential effects of FGF21 on atherosclerosis development through modulation of plasma lipid metabolism.

The main objective of the current study was to evaluate the role of lipoprotein metabolism in the effects of pharmacological FGF21 treatment on atherosclerosis development. To that end, we used APOE*3-Leiden.CETP mice, a translational model for human-like lipoprotein metabolism that, in favourable contrast to ApoE or low-density lipoprotein receptor (LDLR)-knockout mice, respond to the cholesterol-lowering effects of lipid-lowering agents.[23] Here, we report that FGF21 decreases hypercholesterolaemia by accelerating TG-rich lipoprotein turnover as a result of activating brown adipose tissue (BAT) and browning of white adipose tissue (WAT), thereby reducing atherosclerotic lesion severity and increasing the atherosclerotic lesion stability index.

2. Methods

2.1 Animals

Female APOE*3-Leiden.CETP mice were obtained as previously described.[24] Mice at the age of 8–12 weeks were housed under standard conditions (22°C; 12/12-h light/dark cycle) with *ad libitum* access to water and a cholesterol-containing Western-type diet (WTD; 0.15% cholesterol and 16% fat; Altromin, Lage, Germany). All mice were acclimatized to housing and WTD for 3 weeks prior to the pharmacological intervention, to raise plasma cholesterol from ~2 mM up to stable levels of ~15 mM that are sufficient to induce atherosclerosis development. Then, based on 4-h fasted plasma lipid levels, body weight, and body composition, these mice were randomized to two treatment groups receiving either recombinant FGF21 (AstraZeneca, 1 mg/kg body weight, according to previous studies[20,25]) or vehicle [0.1% BSA in sterile-filtered phosphate buffered saline (PBS)] via subcutaneous injection, 3 times per week (i.e. Monday, Wednesday and Friday at 1 pm). In a first study, mice were treated for 16 weeks, in which indirect calorimetry was assessed at week 8 and atherosclerosis development at week 16 ($n = 16$ mice per group). In a second study, mice were treated for 12 weeks, in which an intraperitoneal glucose tolerance test (IPGTT) was performed at week 6 and very low-density lipoprotein (VLDL) production was assessed at week 12 ($n = 8$ per group). Unless indicated otherwise, mice were group housed (3–5 per cage) during the treatment period to avoid stress caused by single housing. In the first study, mice were euthanized with CO_2 inhalation, and in the second study, mice were euthanized with cervical dislocation. All animal experiments were carried out according to the Institute for Laboratory Animal Research Guide for the Care and Use of Laboratory Animals, and were approved by the National Committee for Animal Experiments (Protocol No. AVD1160020173305) and by the Ethics Committee on Animal Care and Experimentation of the Leiden University Medical Center (Protocol No. PE.18.034.014 and No. PE.18.034.044). All animal procedures were conformed the guidelines from Directive 2010/63/EU of the European Parliament on the protection of animal used for scientific purposes.

2.2 Recombinant FGF21 protein

FGF21 has a short half-life *in vivo*, and a Fc-fusion was designed to increase circulation levels for longer duration of action.[26] Recombinant FGF21 protein was generated as described under Expanded Methods in the Supplementary material online.

2.3 Measurement of body weight and body composition

Body weight was determined weekly with a scale, and body composition was determined biweekly in conscious mice using an EchoMRI-100 analyzer (EchoMRI, Houston, TX, USA).

2.4 Indirect calorimetry

In the first experiment, indirect calorimetry was carried out in fully automated metabolic cages (Promethion line, Sable Systems International, Las Vegas, NV, USA) after 8 weeks of treatment. Mice ($n = 8$ per group) were single housed and acclimatized to the system for 48 h, then further monitored for 72 h (3 light/dark cycles). Food intake, physical activity, O_2 consumption (mL/h/kg body weight), and CO_2 production (mL/h/kg body weight) were continuously monitored. Mice had *ad libitum* access to food and water and received either FGF21 or vehicle every other day. Energy expenditure, fat oxidation rate, and carbohydrate oxidation rate were calculated[27] and expressed per mouse. Besides, these values were expressed per g lean mass.

2.5 Glucose tolerance test

In the second experiment, after 6 weeks of treatment, an IPGTT was conducted with an injection of D-glucose (2 g/kg body weight) after 4 h fasting (9:00–13:00; $n = 8$ per group). The IPGTT was performed as described under Expanded Methods in the Supplementary material online. Homoeostasis Model Assessment for Insulin Resistance (HOMA-IR) was calculated with the following formula: [fasting serum glucose (mM) × fasting serum insulin (μU/ml)]/22.5.

2.6 *In vivo* plasma decay and organ uptake of VLDL-mimicking particles

VLDL-mimicking particles (average size 80 nm) labelled with glycerol tri[^{3}H]oleate ([^{3}H]TO) and [^{14}C]cholesteryl oleate ([^{14}C]CO) were prepared using a previously published method.[28] After 16 weeks of treatment, eight mice per group were selected and fasted for 4 h (9:00–13:00) and intravenously injected ($t = 0$ min) with the VLDL-mimicking particles (1.0 mg TG in 200 μL PBS). Blood samples were collected from the tail vein at 0 min (before injection) and 2, 5, 10, and 15 min after injection to measure the plasma decay of [^{3}H]TO and [^{14}C]CO. After 15 min, all mice were sacrificed by CO_2 inhalation and perfused with ice-cold PBS. Subsequently, tissues were isolated, and pieces from the mice treated with VLDL-mimicking particles were transferred into High Performance glass vials (PerkinElmer, Groningen, The Netherlands) and dissolved overnight at 56°C in 0.5 mL Solvable (PerkinElmer, Groningen, The Netherlands). Dissolved organs were mixed with 5 mL Ultima Gold scintillation fluid (PerkinElmer, Groningen, The Netherlands), and vials were placed in a Tri-Carb 2910TR Low Activity Liquid Scintillation Analyzer (PerkinElmer, Groningen, The Netherlands) to assess ^{3}H and ^{14}C activity. Disintegrations per minute (dpm) of ^{3}H and ^{14}C were expressed as percentage of the injected dose per gram tissue. Other pieces of the tissues were either snap-frozen in liquid N_2 (for molecular analysis) or embedded in paraffin (for immunohistochemistry).

2.7 Plasma lipid profiles and adiponectin levels

Every 4 weeks, after 4-h fasting (9:00–13:00), tail vein blood was collected into paraoxon-coated glass capillaries. Plasma was collected and measured for TG, free fatty acid (FFA), and total cholesterol (TC) levels using commercial enzymatic kits from Roche Diagnostics (Mannhein, Germany). Plasma high-density lipoprotein cholesterol (HDL-C) levels were measured using previously published approach.[27] Plasma adiponectin was measured before (week 0) and after (week 16) the treatment using Mouse Adiponectin/Acrp30 Quantikine ELISA Kit (R&D Systems, Minneapolis, NE, USA).

2.8 Adipose tissue histology

Formalin-fixed paraffin-embedded interscapular brown adipose tissue (iBAT) and subcutaneous white adipose tissue (sWAT) tissue sections (5 μm) were prepared for haematoxylin and eosin staining using standard protocols,[29] and uncoupling protein-1 (UCP-1) immunostaining as described previously.[30] The areas occupied by intracellular lipid vacuoles and UCP-1 protein within the iBAT were quantified using Image J software (version 1.52a; National Institutes of Health, Bethesda, Maryland).

2.9 Liver histology and lipid measurements

Formalin-fixed paraffin-embedded liver samples were stained with haematoxylin and eosin staining. The areas occupied by intracellular lipid vacuoles were quantified using Image J software. Hepatic lipids were extracted from frozen liver samples using a modified protocol from Bligh and Dyer.[31] Using commercial kits, TG, TC, and phospholipid (PL) (Instruchemie, Delfzijl, The Netherlands) and protein (Pierce, Thermo Fisher Scientific, Waltham, MA, USA) concentrations were determined. Hepatic lipids were expressed as nmol lipid per mg protein.

2.10 Gene expression analysis

Using Tripure RNA isolation reagent (Roche, Mijdrecht, The Netherlands), total RNA was extracted from snap-frozen tissues. Using Moloney Murine Leukemia Virus Reverse Transcriptase (Promega, Leiden, The Netherlands), complementary DNA for quantitative reverse transcriptase-PCR was generated by reverse transcription of total RNA. Then, mRNA expression was normalized to *β-actin* and *Rplp0* mRNA levels and expressed as fold change compared with the vehicle group. Primer sequences are listed in the Supplementary material online.

2.11 Hepatic VLDL production

In the second experiment, at week 12, mice ($n = 8$) were fasted for 4 h (9:00–13:00) and anaesthetized by the intraperitoneal injection (once) of 6.25 mg/kg Acepromazine (Alfasan, Woerden, The Netherlands), 6.25 mg/kg Midazolam (Roche, Mijdrecht, The Netherlands), and 0.31 mg/kg Fentanyl (Janssen-Cilag, Tilburg, The Netherlands).[32] Anaesthesia was maintained by intraperitoneal injection (three times; every 45 min) of 0.03 mg/kg Acepromazine, 0.03 mg/kg Midazolam, and 0.001 mg/kg Fentanyl.[32] To ensure a proper deep plane of anaesthesia throughout the experimental procedure, the reflexes of mice were checked by pinching the toes of the foot, and body temperature was monitored and maintained using a heating pad. Hepatic VLDL production was assessed as described under Expanded Methods in the Supplementary material online. Commercial kits were used for the measurement of VLDL-TG, -TC, and -PL and -protein.

2.12 Atherosclerosis quantification

In the first experiment, at 16 weeks, hearts were collected, prepared, and cross-sectioned (5 µm) as described previously.[27] Four sections with 50 µm intervals were used per mouse for atherosclerosis measurements. Sections were stained with haematoxylin–phloxine–saffron for histological analysis using standard protocols.[33] Lesions were classified by severity according to the guidelines of the American Heart Association adapted for mice.[34] Various types of lesions were discerned: no lesions, mild lesions (types 1–3), and severe lesions (types 4–5). Lesion composition was assessed as described under Expanded Methods in the Supplementary material online. Lesion area and composition were measured using Image J software. By dividing the relative collagen and smooth muscle cell area by the relative area of macrophages within the same lesion, the stability index was calculated.

2.13 Statistical analyses

Comparisons between vehicle and FGF21 groups were performed using the unpaired two-tailed Student's *t*-test. The square root of the lesion area was taken to linearize the relationship with the plasma TC, non-HDL-C, and HDL-C exposures and plasma adiponectin levels (at 16 weeks). To assess significant correlations between atherosclerotic lesion size and plasma TC, non-HDL-C and HDL-C exposures and plasma adiponectin levels, univariate regression analyses were performed. Then, to predict the contribution of plasma TC, non-HDL-C, and HDL-C exposures and adiponectin to the atherosclerotic lesion size, multiple regression analysis was performed. Data are presented as mean ± SEM, and a *P* value less than 0.05 is considered statistically significant. All statistical analyses were performed with GraphPad Prism 8 (GraphPad Software Inc., CA, USA) except for univariate and multiple regression analyses which were performed with SPSS 20.0 (SPSS, Chicago, IL USA) for Windows.

3. Results

3.1 FGF21 decreases body fat mass by increasing energy expenditure

We first examined whether FGF21 confers its beneficial effect on body weight under atherogenic conditions. In line with previous studies,[4] FGF21 potently prevented weight gain (*Figure 1A*). The body weight of FGF21-treated mice was reduced compared to vehicle-treated mice after only 2 weeks of treatment (-12%) and thereafter stabilized but remained significantly lower (-19% at week 16) than that of vehicle-treated mice. FGF21 only marginally but significantly reduced body lean mass (-6%) after 2 weeks of treatment, which stabilized during the remainder of the treatment period (Supplementary material online, *Figure S1A*). In contrast, FGF21-treated mice showed resistance to gain body fat on the WTD, resulting in a lower fat mass (-46% at week 16) when compared to the vehicle counterparts (*Figure 1B*). Therefore, the reduction of the body weight was mainly caused by fat mass loss. To understand how FGF21 potently reduces fat mass, next we housed mice in metabolic cages to measure whole-body energy metabolism. FGF21 treatment did not influence food intake (*Figure 1C*), nor physical activity (*Figure 1D*). Rather, FGF21 treatment induced a robust and consistent increase in energy expenditure (*Figure 1E* and Supplementary material online, *Figure S2A*), explained mainly by markedly increased fat oxidation (*Figure 1F and G* and Supplementary material online, *Figure S2B–D*), which thus explains the potent effect of FGF21 treatment on preventing fat mass gain.

3.2 FGF21 promotes brown fat activation and white fat browning, and improves glucose metabolism

Since the markedly increased FA oxidation is consistent with BAT activation,[27] we next quantified intracellular lipid vacuoles and UCP-1 abundance in both BAT and WAT. As compared to vehicle group, FGF21 administration reduced iBAT weight (-21%; *Figure 2A*), lowered the lipid droplet content in iBAT (-56%; *Figure 2B*), and increased UCP-1 content in iBAT (+32%; *Figure 2C*), which is consistent with BAT activation. Likewise, FGF21 decreased gonadal WAT (-53%; *Figure 2D*). Since browning predominantly occurs in sWAT,[35] histological analysis was thus performed in sWAT. FGF21 markedly reduced lipid droplet size and increased the number of UCP-1 positive areas (*Figure 2E*), which may suggest that FGF21 improves mitochondrial function in WAT. In line with this suggestion, FGF21 up-regulated the expression of key genes involved in mitochondrial biogenesis and dynamics (*Figure 2F*). Since mitochondrial dysfunction in adipocytes is the primary cause of adipose tissue inflammation,[36] we hypothesized that FGF21 would reduce inflammation in WAT. Indeed, FGF21 decreased mRNA levels of tumour

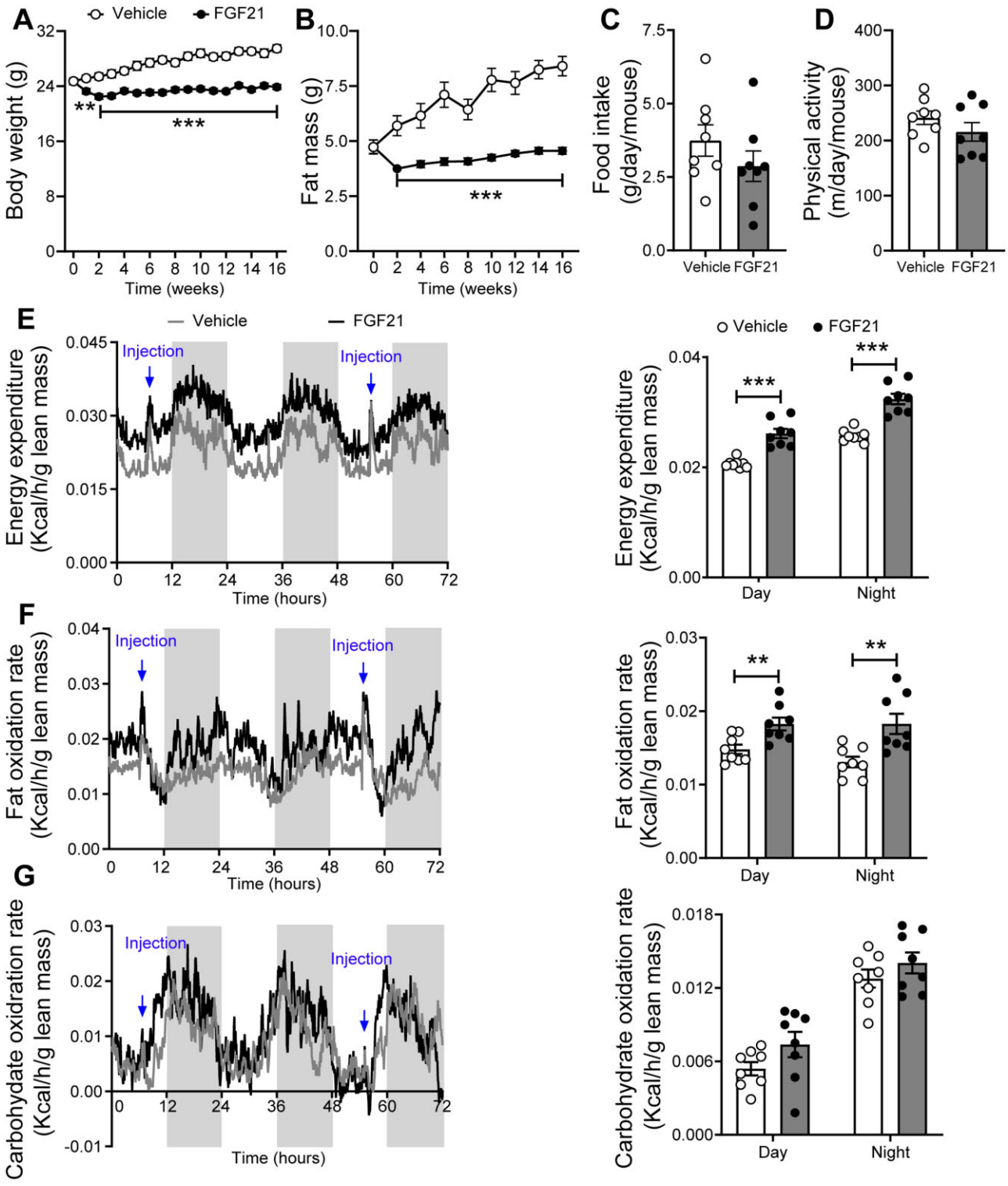

Figure 1 FGF21 decreases body fat mass by increasing energy expenditure. Body weight (*A*) and fat mass (*B*) were measured throughout the study ($n = 15–16$). In week 8, food intake (*C*), physical activity (*D*), energy expenditure (*E*), fat oxidation rate (*F*), and carbohydrate oxidation rate (*G*) were monitored, and values shown (*E–G*) were corrected for body lean mass ($n = 8$). (*A–D*) Data are represented as mean ± SEM. (*E–G*) For line graphs, data are shown as mean for each group (12-h cycle; shaded area represents the dark cycle); for bar graphs, data are shown as mean ± SEM. Differences were assessed using unpaired two-tailed Student's *t*-test. $^{**}P < 0.01$, $^{***}P < 0.001$.

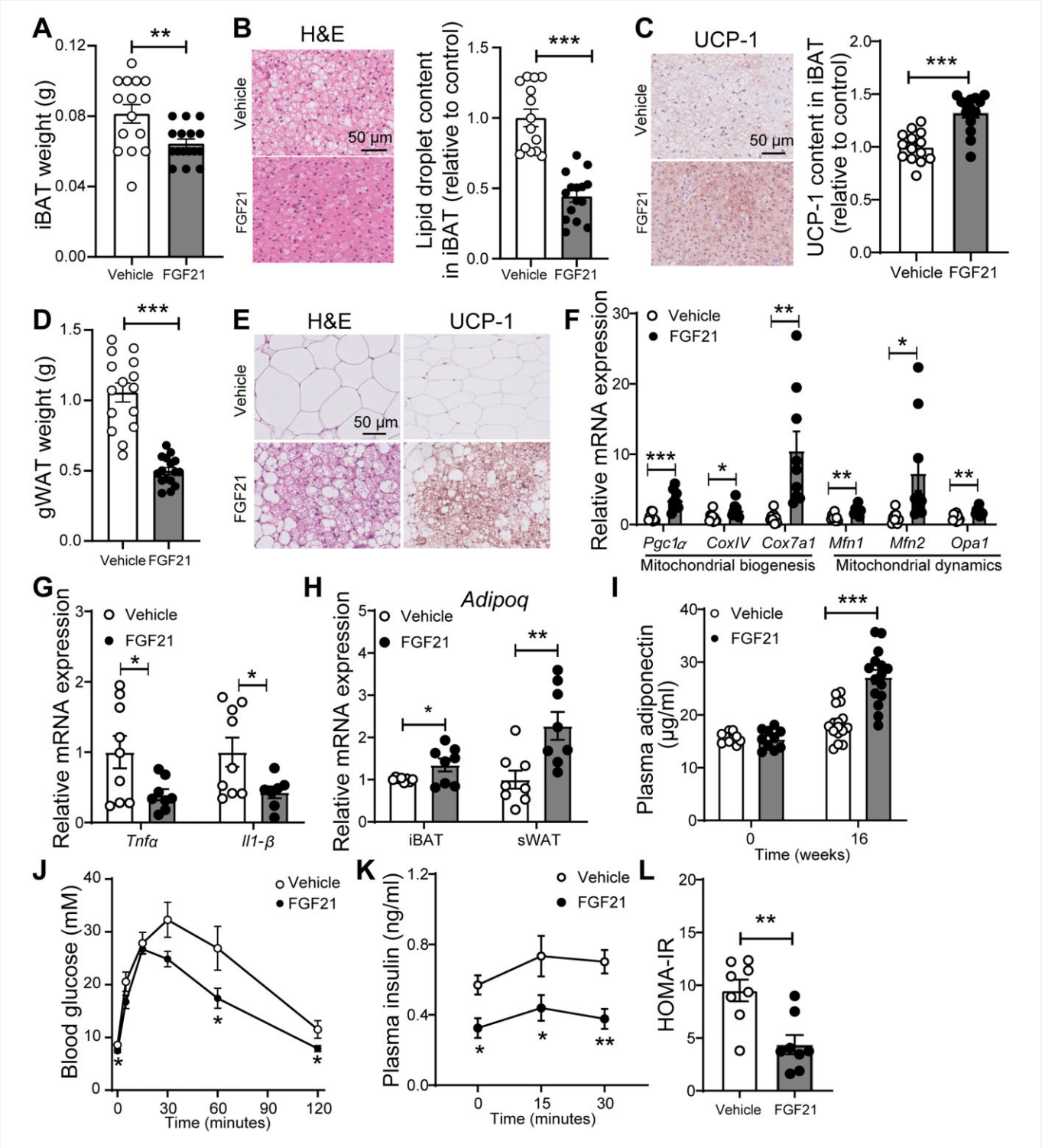

Figure 2 FGF21 promotes brown fat activation and white fat browning, and improves glucose metabolism. After 16 weeks of treatment, interscapular BAT (iBAT) (*A*) and gonadal WAT (gWAT) (*D*) were weighed. In iBAT, the lipid content (*B*) and expression of uncoupling protein-1 (UCP-1) (*C*) were quantified after haematoxyline & eosin (H&E) staining and UCP-1 immunostaining, respectively. The browning of subcutaneous WAT (sWAT) was determined by H&E staining and UCP-1 immunostaining, and representative pictures are shown (*E*). The relative expression of genes involved in mitochondrial function (*F*) and inflammation (*G*) in sWAT, and the relative mRNA levels of *adiponectin* in iBAT and sWAT (*H*) were measured. Fasting plasma adiponectin levels were measured at week 0 and week 16 (*I*). The intraperitoneal glucose tolerance test (IPGTT) was performed after 6 weeks of the treatment, during which plasma glucose (*J*) and insulin (*K*) levels were measured. In addition, the homoeostatic model assessment for insulin resistance (HOMA-IR) was calculated (*L*). Data are represented as mean ± SEM (*A–D*, $n = 14–16$; *F–H*, $n = 8–9$; *I*, $n = 10$ or 15–16; J–L, $n = 7–8$). (*A–I*), data were obtained from the first experiment; (*J–L*), data were obtained from the second experiment. $^*P < 0.05$; $^{**}P < 0.01$, $^{***}P < 0.001$ (unpaired two-tailed Student's *t*-test). *Adipoq*, adiponectin; *CoxIV*, mitochondrial cytochrome C oxidase subunit IV; *Cox7a1*, cytochrome C oxidase polypeptide 7A1; *Il1-β*, interleukin 1 β; *Mfn1/2*, mitofusin-1/2; *Mttp*, microsomal triglyceride transfer protein; *Opa1*, dynamin-like 120 kDa protein, mitochondrial; *Pgc1α*, peroxisome proliferator-activated receptor γ coactivator 1-α; *Tnfα*, tumour necrosis factor α.

necrosis factor α (*Tnfα*; -60%) and Interleukin 1β (*Il1-β*; -57%) in sWAT (*Figure 2G*).

Notably, FGF21 increased adiponectin (*Adipoq*) gene expression in iBAT (+35%), and sWAT (+66%) (*Figure 2H*), accompanied by increased adiponectin levels in the circulation (+47%; *Figure 2I*). Since increased adiponectin was shown to mediate the effect of FGF21 on glucose homoeostasis and insulin sensitivity,[37] an IPGTT was performed in mice in a second experiment after 6 weeks of treatment. FGF21 slightly but significantly reduced fasting blood glucose levels (*Figure 2J*), decreased the glucose excursion during the IPGTT, and lowered plasma insulin levels (*Figure 2K*). Consistently, FGF21 decreased the HOMA-IR index (*Figure 2L*), indicating that FGF21 increases insulin sensitivity also under atherogenic conditions.

3.3 FGF21 promotes TG-derived FA uptake by both brown and white fat and accelerates cholesterol-enriched remnant clearance by the liver

To investigate the role of BAT activation and WAT browning in VLDL metabolism, we intravenously injected mice with VLDL-mimicking particles labelled with [^{3}H]TO and [^{14}C]CO at the end of the study. In vehicle-treated mice, the plasma decay of [^{3}H]TO ($t_{1/2}$ = 5.0 min; *Figure 3A*) was faster than of [^{14}C]CO ($t_{1/2}$ > 15 min; *Figure 3C*), indicating that VLDL-TG-derived FA uptake precedes the clearance of VLDL remnants. While BAT was relatively the most active tissue responsible for the uptake of [^{3}H]TO-derived [^{3}H]oleate (*Figure 3B*), [^{14}C]CO was mainly effectively taken up by the liver (*Figure 3D*). FGF21 largely accelerated the clearance of [^{3}H]TO from plasma ($t_{1/2}$ = 3.5 min; *Figure 3A*) caused by a strongly increased uptake of [^{3}H]TO-derived [^{3}H]oleate by iBAT (+259%), subscapular BAT (+261%), and sWAT (+66%) (*Figure 3B*). Concomitantly, FGF21 treatment accelerated the plasma clearance of [^{14}C]CO ($t_{1/2}$ = 8.5 min; *Figure 3C*). This was mainly attributed to largely increased uptake of [^{14}C]CO by the liver (+128%), although higher [^{14}C]CO uptake was also observed in iBAT (+159%), subscapular BAT (+157%) and sWAT (+95%) (*Figure 3D*). These effects were accompanied by increased hepatic expression of the *Ldlr* (Supplementary material online, *Figure S3A*) and proprotein convertase subtilisin/kexin 9 (*Pcsk9*) (Supplementary material online, *Figure S3B*).

3.4 FGF21 reduces hypercholesterolaemia

We next evaluated the effect of FGF21 on plasma lipid levels. FGF21 increased fasting plasma FFA levels during the first 8 weeks of treatment (*Figure 4A*), reflecting enhanced lipolysis in WAT, followed by an increase in fasting plasma TG levels from week 12 onwards (*Figure 4B*). In contrast, FGF21 consistently decreased fasting plasma TC (*Figure 4C*) and non-HDL-C (*Figure 4D*) levels, and increased fasting plasma HDL-C levels after 16 weeks (*Figure 4E*), indicating that FGF21 improves hypercholesterolaemia under atherogenic conditions.

3.5 FGF21 reduces hepatic steatosis accompanied by up-regulated expression of genes involved in fatty acid oxidation and increased VLDL production

To elucidate the molecular mechanism responsible for FGF21-induced increase of plasma TG levels, we first quantified the hepatic expression of genes involved in lipid handling in livers obtained after 16 weeks. FGF21 up-regulated mRNA expression of the fatty acid transporter, cluster of differentiation 36 (*Cd36*) (*Figure 5A*), accompanied by up-regulated expression of genes involved in *de novo* lipogenesis, including acetyl-CoA carboxylase (*Acc1*), fatty acid synthase (*Fasn*), and diacylglycerol O-acyltransferase 2 (*Dgat2*) (*Figure 5B*). FGF21-treated mice also showed higher hepatic mRNA levels of carnitine palmitoyl transferase 1a (*Cpt1*) and peroxisome proliferator-activated receptor α (*Pparα*), both involved in hepatic FA oxidation (*Figure 5C*).

Interestingly, FGF21 also increased hepatic expression of microsomal triglyceride transfer protein (*Mttp*) and *ApoB* (*Figure 5D*), suggesting that FGF21 increases hepatic VLDL production. Indeed, FGF21 increased both the production rate of VLDL-TG (*Figure 5E*) and VLDL-ApoB (*Figure 5F*). Moreover, FGF21 decreased the amount of TC per ApoB (Supplementary material online, *Figure S4A*) and did not affect the amounts of TG, PL, and protein per ApoB (Supplementary material online, *Figure S4B–D*), suggesting that FGF21-induced increase in plasma TG is due to the increased hepatic VLDL particle production rather than enhanced VLDL lipidation.

Next, to evaluate the effects of FGF21 on hepatic lipid content, histological and biochemical analyses were performed. In line with previous work,[5] FGF21 reduced hepatic steatosis as evidenced by reduced intracellular lipid vacuoles within the liver (-34%; *Figure 5G*) and decreased levels of hepatic TG (-10%), TC (-32%), and PL (-7%) (*Figure 5H*). Consistently, FGF21 reduced liver weight (-36%; *Figure 5I*). Lipid homoeostasis has been shown to play a pivotal role in regulating the inflammatory response in the liver.[38] In line, FGF21 reduced the hepatic mRNA levels of *F4/80, Tnfα,* and monocyte chemoattractant protein-1 (*Mcp-1*) (*Figure 5J*). Collectively, these data suggest that FGF21 increases hepatic FA uptake coupled to enhanced FA oxidation, TG synthesis, and VLDL-TG production, which may together explain the FGF21-induced reduction in steatosis.

3.6 FGF21 attenuates atherosclerosis progression as mainly predicted by the reduction of plasma non-HDL-C levels

Since FGF21 improved hypercholesteraemia, the most important risk factor for atherosclerosis, we next investigated whether FGF21 alleviates atherosclerosis progression. To this end, in the first experiment, atherosclerotic lesion area, severity and composition were determined after 16 weeks of treatment. Histological evaluation showed that FGF21 markedly decreased atherosclerotic lesion area throughout the aortic root (*Figure 6A and B*), leading to a much lower mean atherosclerotic lesion area (-73%; *Figure 6C*). Moreover, FGF21 markedly improved lesion severity as evident from less severe lesions (-74%; *Figure 6D*), more mild lesions (+68%; *Figure 6D*), and more non-diseased segments (+440%; *Figure 6E*). Notably, FGF21 significantly improved atherosclerotic stability index (+46%; *Figure 6G*) via reducing macrophage content (-24%; *Figure 6F and H*) without influencing collagen and smooth muscle cell content within the plaques (Supplementary material online, *Figure S5A* and *B* and *Figure 6H*). Consistently, although the gene expression in aorta tissue of vascular cell adhesion protein 1 (*Vcam-1*) was comparable between these two groups, FGF21-treated mice had lower mRNA levels of intercellular adhesion molecule-1 *(Icam-1*; -41%*)* and *Mcp-1* (-39%) than the control group (*Figure 6I*).

Next, we evaluated the contribution of FGF21-induced TC and non-HDL-C lowering to the attenuation in atherosclerosis. Univariate regression analysis revealed that the lesion area was predicted by plasma TC (R^2 = 0.719) and non-HDL-C (R^2 = 0.706) but not HDL-C (P = 0.307; R^2 = 0.037) (*Figure 6J–L*). Although a previous study showed that

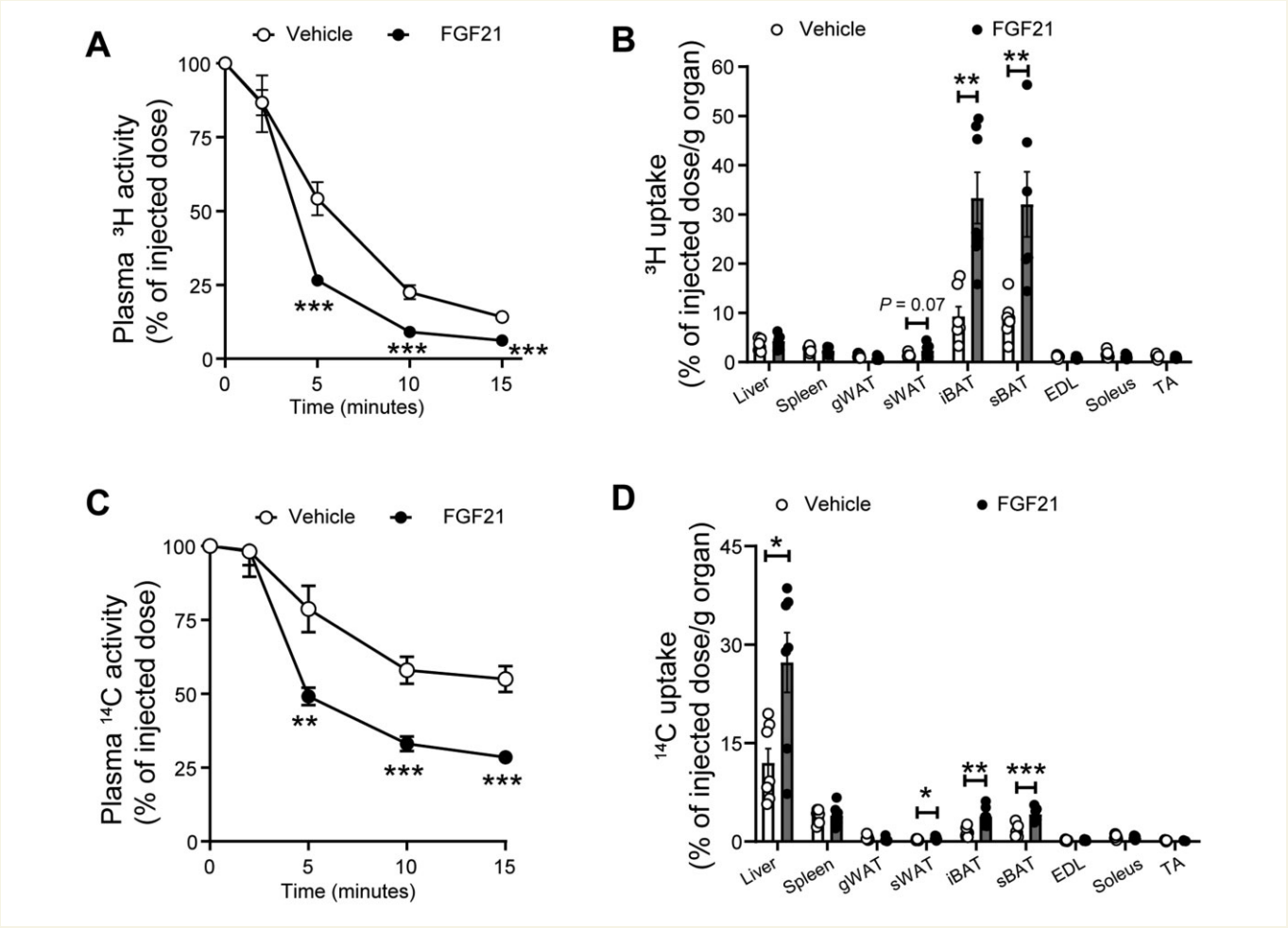

Figure 3 FGF21 promotes TG-derived FA uptake by brown fat and white fat and accelerates cholesterol-enriched remnant clearance by the liver. The clearance of ^{3}H (*A*) and ^{14}C (*C*) from plasma and the uptake of ^{3}H (*B*) and ^{14}C (*D*) by various tissues were assessed. Data are represented as mean ± SEM ($n = 6$–7). *$P < 0.05$, **$P < 0.01$, ***$P < 0.001$ (unpaired two-tailed Student's *t*-test). EDL, extensor digitorum longus; gWAT, gonadal white adipose tissue; iBAT, interscapular brown adipose tissue; sBAT, subscapular brown adipose tissue; sWAT, subcutaneous white adipose tissue; TA, tibialis anterior.

adiponectin can mediate the FGF21-induced reduction of atherosclerosis,[19] we observed that plasma adiponectin levels predicted lesion area to only a modest extent ($P = 0.005$; $R^2 = 0.259$; *Figure 6M*). Taken together, in our experimental model FGF21 reduces atherosclerosis mainly by reducing non-HDL-C.

4. Discussion

FGF21 has been proposed to be a physiological protector against metabolic stress, while pharmacological doses of FGF21 mimetics to animal models or human lead to profound effects on insulin sensitivity and lipid profile.[39] Although clinical trials are underway with long-acting analogs of FGF21 to combat obesity, type 2 diabetes, and non-alcoholic steatohepatitis,[40] the effect of pharmacological treatment with FGF21 on atherosclerosis development as well as underlying mechanisms are far from being elucidated. Here, we used APOE*3-Leiden.CETP mice to show that exogenous recombinant FGF21 primes adipose tissue to enhance VLDL-TG hydrolysis and uptake of liberated FA by BAT and WAT, followed by accelerated uptake of cholesterol-enriched remnants by the liver. Accordingly, FGF21 markedly reduces circulating atherogenic cholesterol levels, thereby potently attenuating atherosclerosis development.

First, we demonstrated that FGF21 also in an atherogenic setting enhances energy expenditure leading to prevention of body fat gain. FGF21-induced weight loss has been reported to be caused in part by the induction of energy expenditure in obese rodents and humans, achieved by the recruitment of thermogenic pathways in brown fat and the browning of white fat.[25,41] Consistently, our histological and immunologic analyses showed that FGF21 treatment markedly increased BAT activation and WAT browning as determined by UCP-1 protein expression. We did not observe any effect of FGF21 on food consumption. In diabetic rhesus monkeys, FGF21 at high doses up to 50 mg/kg did decrease food intake up to 60%, contributing to body weight lowering.[21] However, FGF21 treatment at lower doses induced weight loss without affecting food intake in wild-type mice,[4] diet-induced obese mice,[5] and non-human primates,[42] which is consistent with our data. Also, in our study FGF21 did not seem to affect physical activity, while FGF21 increased physical activity in diet-induced obese mice[5] and stimulated torpor in 24 h-fasted wild-type mice.[8] These seemingly divergent results

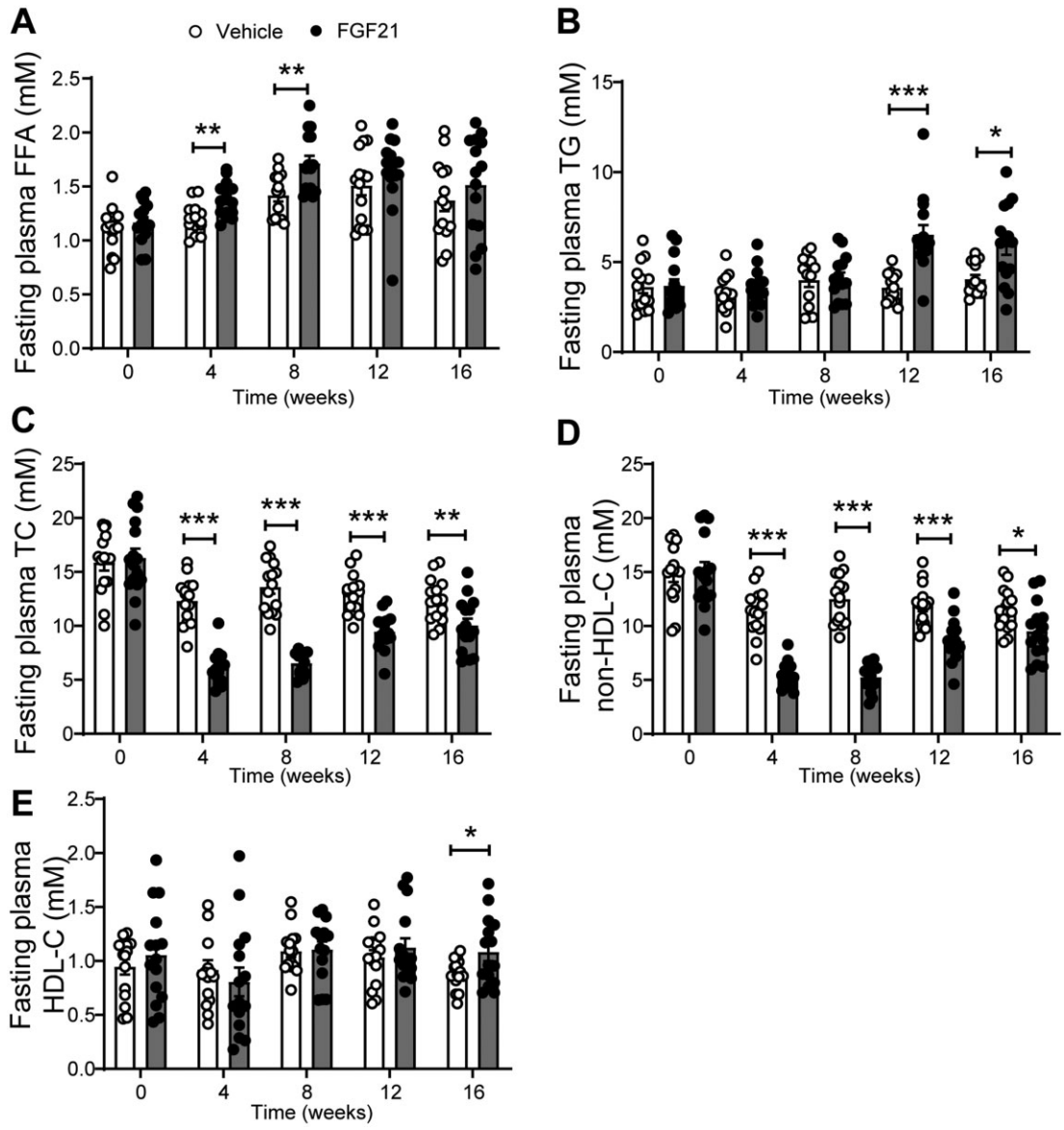

Figure 4 FGF21 reduces hypercholesterolaemia. Throughout the study, fasting plasma levels of free fatty acids (FFA) (*A*), triglycerides (TG) (*B*), total cholesterol (TC) (*C*), non-high density lipoprotein-cholesterol (non-HDL-C) (*D*) and high density lipoprotein-cholesterol (HDL-C) (*E*) were measured. Data are represented as mean ± SEM ($n = 14$–15). *$P < 0.05$, **$P < 0.01$, ***$P < 0.001$ (unpaired two-tailed Student's *t*-test).

suggest a critical role of FGF21 in maintaining energy homoeostasis. At least, in our lean APOE*3-Leiden.CETP mice treated with moderate pharmacological doses of FGF21 (1 mg/kg; three times per week), prevention of body fat gain is thus mainly attributed to enhanced energy expenditure. The fact that we observed enhanced oxidation of FAs versus carbohydrates is in line with selective classical BAT activation as induced by cold exposure or β3-adrenergic receptor activation in both mice and humans.[27,43–45] Additionally, we observed that FGF21 slightly prevented lean body mass gain. Although we did not perform detailed studies to investigate the specific organs affected, this may be attributed to a generally increased catabolic state induced by FGF21.

We also showed that FGF21 improves glucose tolerance and insulin sensitivity under atherogenic conditions. A previous study showed that the metabolic effects of FGF21 on glucose homoeostasis and insulin sensitivity are mediated by adiponectin.[37] Consistently, in our study FGF21 up-regulated adiponectin expression in both BAT and WAT, accompanied by highly increased plasma adiponectin levels. We also showed that FGF21 reduced inflammation in WAT, through which insulin sensitivity may have improved.[36] In white adipocytes, mitochondrial function has been reported to be essential for adiponectin synthesis,[46,47] and mitochondrial dysfunction has been postulated as the primary cause of adipose tissue inflammation.[36] Therefore, the beneficial effects of FGF21 on glucose metabolism may be attributed to an improvement of WAT mitochondrial function, which is in agreement with our findings.

Next, we reported that FGF21 alleviates WTD-induced hypercholesterolaemia, with a marked initial reduction of non-HDL-C levels and increased HDL-C levels after prolonged intervention. This is in agreement with human studies showing that administering either FGF21 or FGF21

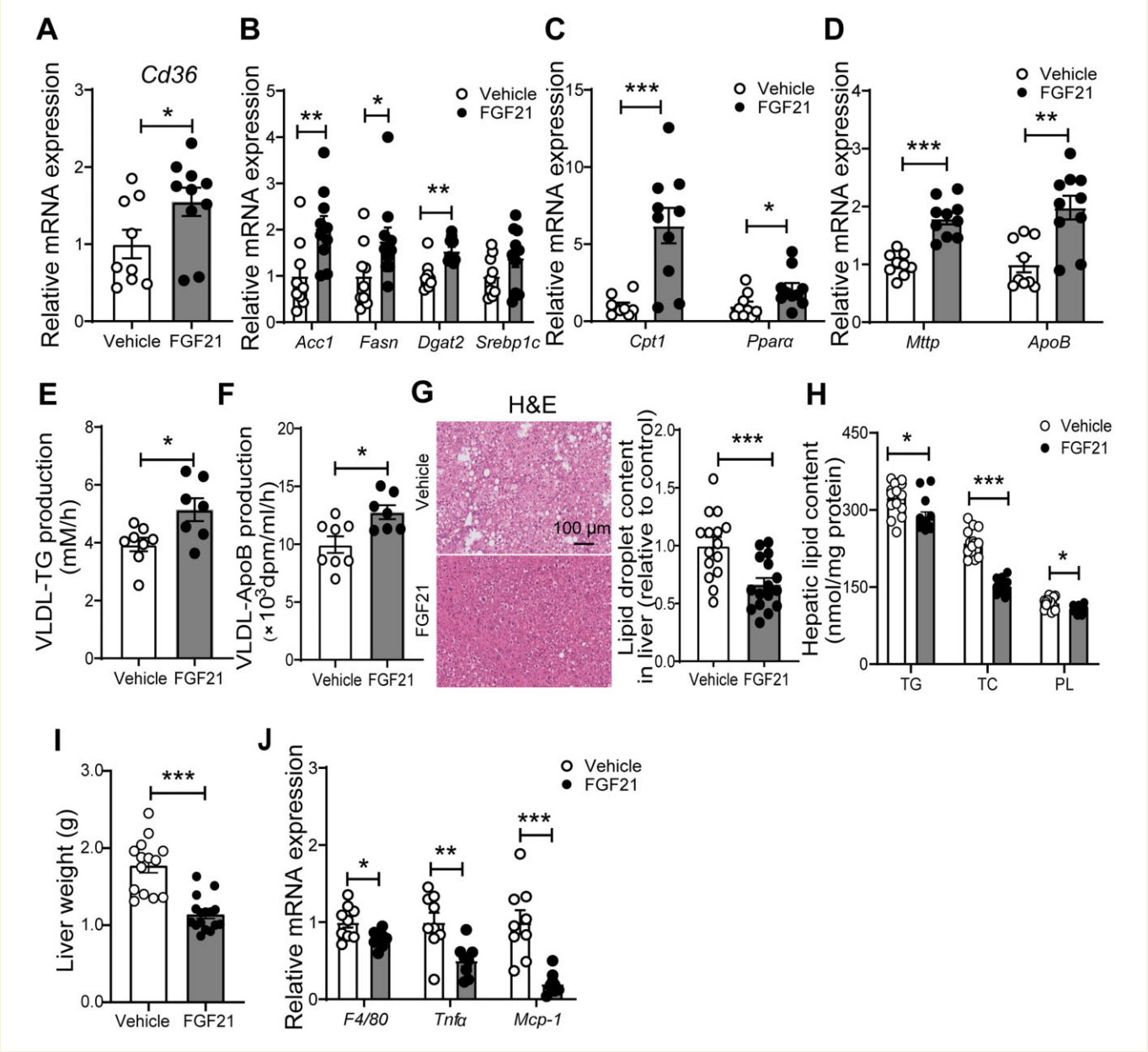

Figure 5 FGF21 reduces hepatic steatosis accompanied by up-regulated expression of genes involved in fatty acid oxidation and increased VLDL particle production. After 16 weeks of treatment, the relative mRNA expression levels of genes involved in fatty acid uptake (*A*), *de novo* lipogenesis (*B*) and fatty acid oxidation (*C*), very low-density lipoprotein (VLDL) production and secretion (*D*) and inflammation (*J*) were determined in the liver. The hepatic VLDL-TG (*E*) and VLDL-ApoB (*F*) production rates were assessed after 12 weeks of the treatment. After 16 weeks of treatment, the hepatic lipid content was assessed by H&E staining (*G*), and triglyceride (TG), total cholesterol (TC), and phospholipid (PL) levels (*H*) were determined within the liver, and liver weight (*I*) was measured. Data are represented as mean ± SEM (A–D and *J*, $n = 8$–10; *E–F*, $n = 7$–8; *G–H*, $n = 14$–16). (*A–D*) and (*G–J*), data were obtained from the first experiment; (*E–F*), data were obtained from the second experiment. $^{*}P < 0.05$, $^{**}P < 0.01$, $^{***}P < 0.001$ (unpaired two-tailed Student's *t*-test). *Acc1*, acetyl-CoA carboxylase; *ApoB*, apolipoprotein B; *Cd36*, cluster of differentiation 36; *Cpt1*, carnitine palmitoyl transferase 1; *Dgat2*, diacylglycerol O-acyltransferase 2; *Fasn*, fatty acid synthase; *Mcp-1*, monocyte chemoattractant protein 1; *Mttp*, microsomal triglyceride transfer protein; *Ppara*, peroxisome proliferator-activated receptor α; *Srebp1c*, sterol regulatory element-binding transcription factor 1; *Tnfα*, tumour necrosis factor α.

analogs improves the plasma lipid profile.[21,48] Mechanistic studies revealed that FGF21 enhances lipolytic conversion of VLDL by BAT and by WAT. Consistently, a clinical trial has shown that FGF21 treatment up-regulated gene/protein expression related to thermogenesis in human adipocyte.[49] Given that our data are in line with classical BAT activation, the increased uptake of liberated FAs by WAT is probably the direct consequence of browning.[27] The avid uptake of generated VLDL remnants resulting from lipolysis by BAT and browned WAT by the liver is likely mediated via the ApoE-LDLR pathway, since we previously observed that clearance of VLDL remnants generated by BAT and

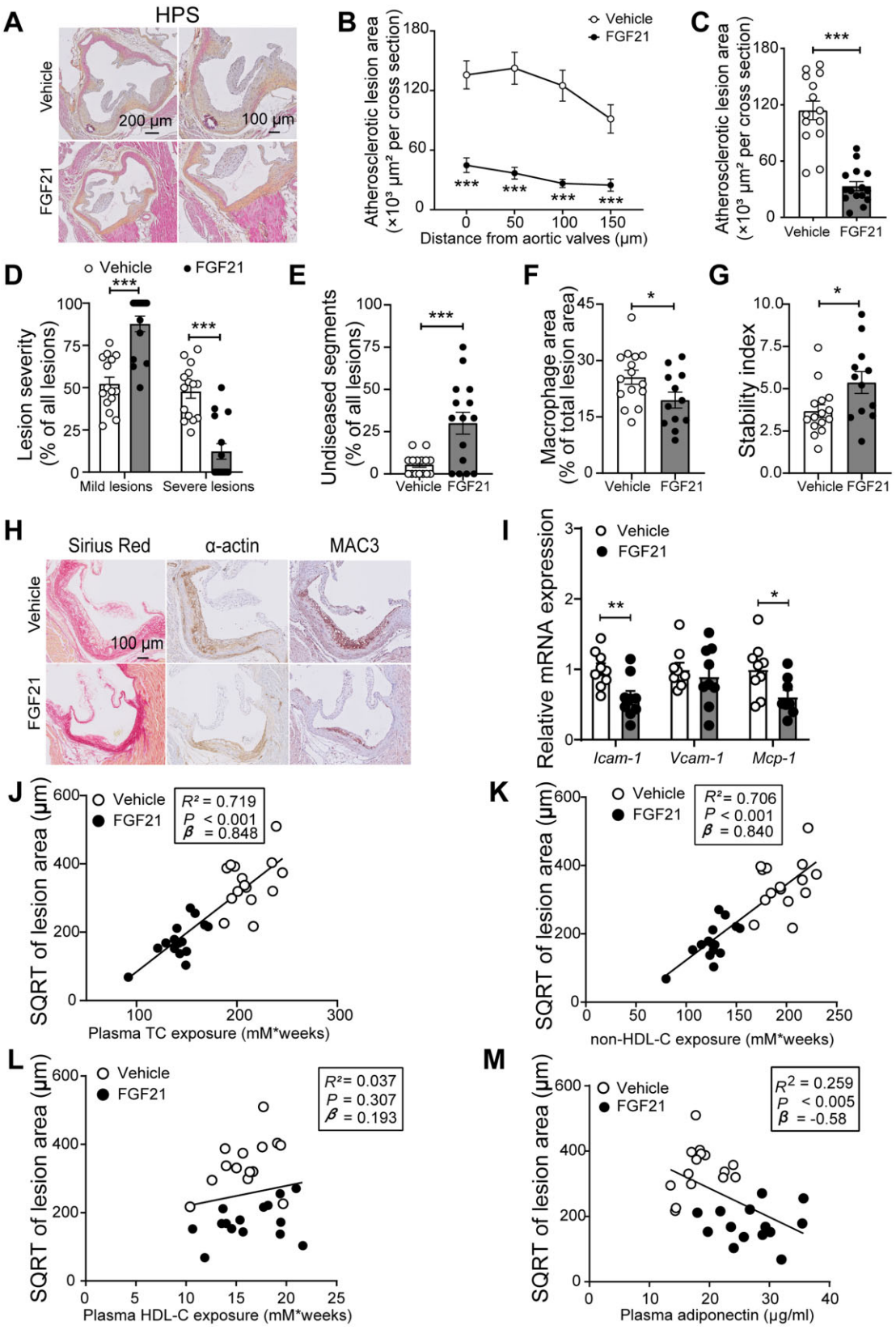

Figure 6 FGF21 protects against atherosclerosis progression as largely predicted by the reduction of plasma non-HDL-C levels. At week 16, hearts were collected, the valve areas of their aortic roots were stained with haematoxylin–phloxine–saffron (HPS), and representative pictures are shown (*A*). Lesion area as a function of distance from the aortic valves was determined by calculating the lesion area of four consecutive cross-sections starting from the appearance of open aortic valve leaflets (*B*). From the four cross-sections, the mean atherosclerotic lesion area was determined (*C*). Lesions were categorized according to lesion severity (*D*), and the percentage of non-diseased segments was scored (*E*). The valve area of aortic root was stained with Sirius Red, an

browned WAT is impaired in ApoE-deficient and LDLR-deficient mice.[27] Consistently, we found that FGF21 treatment markedly increased hepatic *Ldlr* expression, albeit that hepatic *Pcsk9* levels were also increased upon FGF21 treatment. Likely, the increase in hepatic *Ldlr* expression aims to compensate for the reduced hepatic cholesterol levels by increasing the uptake of cholesterol from the circulation, while *Pcsk9* regulates *Ldlr* expression to maintain the homoeostasis of this process. However, in contrast to classical BAT activation, we did not observe a lowering in plasma TG, which was even increased by prolonged FGF21 treatment. Notably, while β3-adrenergic receptor activation did not increase plasma FFA,[27] FGF21 increased FFA levels already after short-term treatment, which has been described as a compensatory mechanism to adapt to the highly increased energy expenditure.[50,51] Therefore, it is likely that FGF21 induces more massive lipolysis in WAT as compared to classical BAT activation, which subsequently induces substrate-driven VLDL production in the liver. This would be in full agreement with the observed increased hepatic expression of genes involved in FA uptake, *de novo* lipogenesis, and VLDL production and increased VLDL-TG production rate.

We also observed that FGF21 treatment reduces hepatic lipid levels. While a high FFA flux to the liver may lead to hepatic steatosis, e.g. as observed in CD36-deficient mice,[52] both TG, TC, and PL levels were lower in FGF21- vs. vehicle-treated mice. Besides that FGF21 increases VLDL production, which already limits accumulation of TG in the liver, FGF21 probably also up-regulates hepatic FA oxidation, further indicating a role of FGF21 in maintaining circulating FFA and hepatic lipid homoeostasis. Interesting, a previous study demonstrated that FGF21 lowers plasma TG by reducing FFA and consequently hepatic VLDL lipidation.[18] This seeming discrepancy with our study is likely explained by different diets and different treatment periods. While our mice received WTD containing 16% fat and FGF21 treatment for 16 weeks, in the study of Schlein et al.,[18] mice were fed a high-fat diet (60% fat) and treated with FGF21 for only 10 days. During a short-term FGF21 intervention period on high-fat diet, the diet may provide sufficient chylomicron-TG to maintain the whole-body energy homoeostasis. As compared to high-fat diet, WTD contains limited TG that may not meet the need for the increased whole-body metabolism, especially during prolonged FGF21 treatment. Moreover, we showed that FGF21 treatment reduces hepatic inflammation, which is consistent with previous studies showing that FGF21 inhibits inflammation during non-alcoholic steatohepatitis development.[40,53]

Finally, we observed that FGF21 treatment markedly reduces atherosclerosis development. Univariate regression analysis revealed that the reduction in atherosclerotic lesion area was mainly predicted by the reduction in non-HDL-C. In line with this, clinical trials have shown that early interventions to lower non-HDL-C levels can reverse and even eradicate earlier stages of atherosclerosis.[1] FGF21 also increased the atherosclerotic plaque stability index via decreasing the lesion macrophage content relative to the smooth muscle cell and collagen content. This may indicate that besides lowering cholesterol to reduce atherosclerosis initiation, FGF21 may also regulate inflammation which would be in agreement with our observation that FGF21 reduces spleen weight (-26.6%; Supplementary material online, *Figure S1B*) and inhibits the expression of the *Icam-1* and *Mcp-1* in the aorta. In addition, FGF21 was shown to regulate foam cell formation and inflammatory responses in oxidized low-density lipoprotein-induced macrophages *in vitro*.[54] A preclinical study showed that adiponectin may mediate the anti-inflammatory effects of FGF21 in atherosclerosis.[19] In line, FGF21 increased adiponectin in our study and plasma adiponectin levels explained ∼26% of the variation in atherosclerotic lesion area. However, adiponectin may not play a protective causal role in coronary heart diseases pathogenesis in humans.[55] From studies using FGF21 deficient ApoE-knockout mice, it was implied that endogenous FGF21 reduces hepatic cholesterol synthesis, thereby protecting against atherosclerosis.[19] In contrast, we found that FGF21 treatment up-regulated the hepatic expression of genes involved in cholesterol synthesis, including 3-hydroxy-3-methylglutaryl-CoA reductase (*Hmgcr*; Supplementary material online, *Figure S3C*) and sterol regulatory element-binding protein-2 (*Srebp2*; Supplementary material online, *Figure S3D*), likely as a compensatory response to decreased cholesterol levels. Since FGF21 has been proposed to play a key role in hepatic cholesterol clearance in wild-type mice,[7] and ApoE-knockout mice have an abrogated hepatic uptake of remnant lipoproteins, these data obtained in ApoE-knockout mice probably have limited translational value for humans.

This study is not without limitations. First, we used recombinant lipoproteins that acquire all exchangeable apolipoproteins but do not have apoB.[28] Nevertheless, our previous studies have shown that they truly mimic TG-rich lipoprotein metabolism in mice, since ApoB is mainly required for their synthesis while ApoE is essential for their clearance. Second, the long-circulating recombinant FGF21 protein may not fully represent the wild-type native protein. However, the *in vitro* activities are comparable between these two proteins (e.g. Erk phosphorylation and βKlotho binding activity),[26] and the main purpose of our study was to explore a pharmacological FGF21-based strategy, for which long-circulating recombinant FGF21 is evidently preferred over short-lived endogenous FGF21.

In conclusion, our present study uncovers that the anti-atherogenic effects of FGF21 are mainly mediated through reducing hypercholesterolaemia. Mechanistically, FGF21 activates BAT and induces browning of WAT, resulting in accelerated catabolism of TG-rich lipoproteins followed by rapid uptake of their remnants by the liver. Given that chronic administration of a long-acting form of FGF21 in obese patients reduces plasma TC and non-HDL-C levels,[21,48] and FGF21 is a biomarker of subclinical atherosclerosis in humans,[56] our study supports the development of FGF21 as a powerful therapeutic for the treatment of hypercholesterolaemia and atherosclerosis.

Figure 6 Continued

anti-α-actin antibody and an anti-MAC3 antibody to quantify the content of collagen, smooth muscle cells, and macrophages (*F*) within the lesions, respectively. Representative pictures are shown (*H*). The stability index (collagen and smooth muscle cell content/macrophage content of the lesions) was calculated (*G*). The relative expression of genes involved in inflammation was measured in aorta (*I*). The square root (SQRT) of the atherosclerotic lesion area was plotted against the plasma TC (*J*), non-HDL-C (*K*) and HDL-C (*L*) exposure during the 16-week treatment period and plasma adiponectin levels at week 16 (*M*). Linear regression analyses were performed. Data are represented as mean ± SEM (*B–E* and *J–M*, $n = 14–15$; *F–G*, $n = 12–15$; *I*, $n = 8–9$). $^{*}P < 0.05$, $^{***}P < 0.001$ (unpaired two-tailed Student's *t*-test). *Icam-1*, intercellular adhesion molecule 1; *Mcp-1*, monocyte chemoattractant protein 1; *Vcam-1*, vascular cell adhesion molecule 1.

Supplementary material

Supplementary material is available at *Cardiovascular Research* online.

Authors' contributions

C.L. designed the study, carried out the research, analysed and interpreted the results, and wrote and revised the manuscript. M.S. carried out the research, interpreted the results, reviewed and revised the manuscript, and obtained the funding. E.Z., Z.L., S.K., and M.R.B. advised the study and reviewed the manuscript. M.L. and K.W. advised the study, interpreted the results, and reviewed the manuscript. N.D. designed long-circulating recombinant FGF21 and edited the manuscript. L.B. synthesized and purified long-circulating recombinant FGF21. X.-R.P. provided long-circulating recombinant FGF21, advised the study, interpreted the results, and reviewed the manuscript. Y.W. designed and advised the study, interpreted the results, reviewed and revised the manuscript, and obtained the funding. P.C.N.R. designed and advised the study, interpreted the results, edited, reviewed, and revised the manuscript and obtained funding.

Acknowledgements

We thank for T.C.M. Streefland, A.C.M. Pronk, and R.A. Lalai from Department of Medicine, the Division of Endocrinology, Leiden University Medical Center for technical assistance.

Conflict of interest: M.L., K.W., N.D., L.B., and X.-R.P. are employees of AstraZeneca.

Data availability

The data underlying this article will be shared on reasonable request to the corresponding author.

Funding

This work was supported by the Dutch Diabetes Research Foundation [2015.81.1808 to M.R.B.]; Chinese Scholarship Council grants [CSC to E.Z. and Z.L.]; the Netherlands Organization for Scientific Research-NWO [VENI grant 91617027 to Y.W.]; the Netherlands Organization for Health Research and Development-ZonMW [Early Career Scientist Hotel grant 435004007 to Y.W.]; the Novo Nordisk Foundation [NNF18OC0032394 to M.S.]; the Netherlands Cardiovascular Research Initiative: an initiative with support of the Dutch Heart Foundation [CVON-GENIUS-2]; and the Netherlands Heart Foundation [2009T038 to P.C.N.R.].

References

1. Robinson JG, Williams KJ, Gidding S, Borén J, Tabas I, Fisher EA, Packard C, Pencina M, Fayad ZA, Mani V, Rye KA, Nordestgaard BG, Tybjærg-Hansen A, Douglas PS, Nicholls SJ, Pagidipati N, Sniderman A. Eradicating the burden of atherosclerotic cardiovascular disease by lowering apolipoprotein B lipoproteins earlier in life. *J Am Heart Assoc* 2018;**7**:e009778.
2. Hegele RA, Gidding SS, Ginsberg HN, McPherson R, Raal FJ, Rader DJ, Robinson JG, Welty FK. Nonstatin low-density lipoprotein-lowering therapy and cardiovascular risk reduction-statement from ATVB council. *Arterioscler Thromb Vasc Biol* 2015;**35**:2269–2280.
3. Reiner Z. Resistance and intolerance to statins. *Nutr Metab Cardiovasc Dis* 2014;**24**:1057–1066.
4. Coskun T, Bina HA, Schneider MA, Dunbar JD, Hu CC, Chen Y, Moller DE, Kharitonenkov A. Fibroblast growth factor 21 corrects obesity in mice. *Endocrinology* 2008;**149**:6018–6027.
5. Xu J, Lloyd DJ, Hale C, Stanislaus S, Chen M, Sivits G, Vonderfecht S, Hecht R, Li YS, Lindberg RA, Chen JL, Jung DY, Zhang ZY, Ko HJ, Kim JK, Veniant MM. Fibroblast growth factor 21 reverses hepatic steatosis, increases energy expenditure, and improves insulin sensitivity in diet-induced obese mice. *Diabetes* 2009;**58**:250–259.
6. Ameka M, Markan KR, Morgan DA, BonDurant LD, Idiga SO, Naber MC, Zhu Z, Zingman LV, Grobe JL, Rahmouni K, Potthoff MJ. Liver derived FGF21 maintains core body temperature during acute cold exposure. *Sci Rep* 2019;**9**:630.
7. Badman MK, Pissios P, Kennedy AR, Koukos G, Flier JS, Maratos-Flier E. Hepatic fibroblast growth factor 21 is regulated by PPARalpha and is a key mediator of hepatic lipid metabolism in ketotic states. *Cell Metab* 2007;**5**:426–437.
8. Inagaki T, Dutchak P, Zhao G, Ding X, Gautron L, Parameswara V, Li Y, Goetz R, Mohammadi M, Esser V, Elmquist JK, Gerard RD, Burgess SC, Hammer RE, Mangelsdorf DJ, Kliewer SA. Endocrine regulation of the fasting response by PPARalpha-mediated induction of fibroblast growth factor 21. *Cell Metab* 2007;**5**:415–425.
9. Dushay J, Chui PC, Gopalakrishnan GS, Varela-Rey M, Crawley M, Fisher FM, Badman MK, Martinez-Chantar ML, Maratos-Flier E. Increased fibroblast growth factor 21 in obesity and nonalcoholic fatty liver disease. *Gastroenterology* 2010;**139**:456–463.
10. Cheng XB, Zhu B, Jiang FS, Fan HY. Serum FGF-21 levels in type 2 diabetic patients. *Endocr Res* 2011;**36**:142–148.
11. Praktiknjo M, Djayadi N, Mohr R, Schierwagen R, Bischoff J, Dold L, Pohlmann A, Schwarze-Zander C, Wasmuth JC, Boesecke C, Rockstroh JK, Trebicka J. Fibroblast growth factor 21 is independently associated with severe hepatic steatosis in non-obese HIV-infected patients. *Liver Int* 2019;**39**:1514–1520.
12. Sanyal A, Charles ED, Neuschwander-Tetri BA, Loomba R, Harrison SA, Abdelmalek MF, Lawitz EJ, Halegoua-DeMarzio D, Kundu S, Noviello S, Luo Y, Christian R. Pegbelfermin (BMS-986036), a PEGylated fibroblast growth factor 21 analogue, in patients with non-alcoholic steatohepatitis: a randomised, double-blind, placebo-controlled, phase 2a trial. *Lancet* 2019;**392**:2705–2717.
13. Ding X, Boney-Montoya J, Owen BM, Bookout AL, Coate KC, Mangelsdorf DJ, Kliewer SA. betaKlotho is required for fibroblast growth factor 21 effects on growth and metabolism. *Cell Metab* 2012;**16**:387–393.
14. Fisher FM, Maratos-Flier E. Understanding the physiology of FGF21. *Annu Rev Physiol* 2016;**78**:223–241.
15. Geller S, Arribat Y, Netzahualcoyotzi C, Lagarrigue S, Carneiro L, Zhang L, Amati F, Lopez-Mejia IC, Pellerin L. Tanycytes regulate lipid homeostasis by sensing free fatty acids and signaling to key hypothalamic neuronal populations via FGF21 Secretion. *Cell Metab* 2019;**30**:833–844 e837.
16. Bookout AL, de Groot MH, Owen BM, Lee S, Gautron L, Lawrence HL, Ding X, Elmquist JK, Takahashi JS, Mangelsdorf DJ, Kliewer SA. FGF21 regulates metabolism and circadian behavior by acting on the nervous system. *Nat Med* 2013;**19**:1147–1152.
17. Huang Z, Zhong L, Lee JTH, Zhang J, Wu D, Geng L, Wang Y, Wong CM, Xu A. The FGF21-CCL11 axis mediates beiging of white adipose tissues by coupling sympathetic nervous system to type 2 immunity. *Cell Metab* 2017;**26**:493–508 e494.
18. Schlein C, Talukdar S, Heine M, Fischer AW, Krott LM, Nilsson SK, Brenner MB, Heeren J, Scheja L. FGF21 lowers plasma triglycerides by accelerating lipoprotein catabolism in white and brown adipose tissues. *Cell Metab* 2016;**23**:441–453.
19. Lin Z, Pan X, Wu F, Ye D, Zhang Y, Wang Y, Jin L, Lian Q, Huang Y, Ding H, Triggle C, Wang K, Li X, Xu A. Fibroblast growth factor 21 prevents atherosclerosis by suppression of hepatic sterol regulatory element-binding protein-2 and induction of adiponectin in mice. *Circulation* 2015;**131**:1861–1871.
20. Kharitonenkov A, Wroblewski VJ, Koester A, Chen YF, Clutinger CK, Tigno XT, Hansen BC, Shanafelt AB, Etgen GJ. The metabolic state of diabetic monkeys is regulated by fibroblast growth factor-21. *Endocrinology* 2007;**148**:774–781.
21. Talukdar S, Zhou YJ, Li DM, Rossulek M, Dong J, Somayaji V, Weng Y, Clark R, Lanba A, Owen BM, Brenner MB, Trimmer JK, Gropp KE, Chabot JR, Erion DM, Rolph TP, Goodwin B, Calle RA. A long-acting FGF21 molecule, PF-05231023, decreases body weight and improves lipid profile in non-human primates and type 2 diabetic subjects. *Cell Metab* 2016;**23**:427–440.
22. Jin L, Lin Z, Xu A. Fibroblast growth factor 21 protects against atherosclerosis via fine-tuning the multiorgan crosstalk. *Diabetes Metab J* 2016;**40**:22–31.
23. van den Hoek AM, van der Hoorn JW, Maas AC, van den Hoogen RM, van Nieuwkoop A, Droog S, Offerman EH, Pieterman EJ, Havekes LM, Princen HM. APOE*3Leiden.CETP transgenic mice as model for pharmaceutical treatment of the metabolic syndrome. *Diabetes Obes Metab* 2014;**16**:537–544.23.
24. Westerterp M, van der Hoogt CC, de Haan W, Offerman EH, Dallinga-Thie GM, Jukema JW, Havekes LM, Rensen PC. Cholesteryl ester transfer protein decreases high-density lipoprotein and severely aggravates atherosclerosis in APOE*3-Leiden mice. *ATVB* 2006;**26**:2552–2559.
25. Samms RJ, Smith DP, Cheng CC, Antonellis PP, Perfield JW, 2nd, Kharitonenkov A, Gimeno RE, Adams AC. Discrete aspects of FGF21 in vivo pharmacology do not require UCP1. *Cell Rep* 2015;**11**:991–999.
26. Hecht R, Li YS, Sun J, Belouski E, Hall M, Hager T, Yie J, Wang W, Winters D, Smith S, Spahr C, Tam LT, Shen Z, Stanislaus S, Chinookoswong N, Lau Y, Sickmier A, Michaels ML, Boone T, Veniant MM, Xu J. Rationale-based engineering of a potent long-acting FGF21 analog for the treatment of type 2 diabetes. *PLoS One* 2012;**7**:e49345.
27. Berbee JF, Boon MR, Khedoe PP, Bartelt A, Schlein C, Worthmann A, Kooijman S, Hoeke G, Mol IM, John C, Jung C, Vazirpanah N, Brouwers LP, Gordts PL, Esko JD,

Hiemstra PS, Havekes LM, Scheja L, Heeren J, Rensen PC. Brown fat activation reduces hypercholesterolaemia and protects from atherosclerosis development. *Nat Commun* 2015;**6**:6356.
28. Rensen PC, van Dijk MC, Havenaar EC, Bijsterbosch MK, Kruijt JK, van Berkel TJ. Selective liver targeting of antivirals by recombinant chylomicrons - a new therapeutic approach to hepatitis-B. *Nat Med* 1995;**1**:221–225.
29. Cardiff RD, Miller CH, Munn RJ. Manual hematoxylin and eosin staining of mouse tissue sections. *Cold Spring Harb Protoc* 2014;**2014**:655–658.
30. Kooijman S, Wang Y, Parlevliet ET, Boon MR, Edelschaap D, Snaterse G, Pijl H, Romijn JA, Rensen PC. Central GLP-1 receptor signalling accelerates plasma clearance of triacylglycerol and glucose by activating brown adipose tissue in mice. *Diabetologia* 2015;**58**:2637–2646.
31. Bligh EG, Dyer WJ. A rapid method of total lipid extraction and purification. *Can J Biochem Physiol* 1959;**37**:911–917.
32. Wang Y, Berbee JF, Stroes ES, Smit JW, Havekes LM, Romijn JA, Rensen PC. CETP expression reverses the reconstituted HDL-induced increase in VLDL. *J Lipid Res* 2011;**52**:1533–1541.
33. Bencosme SA. A trichrome staining method for routine use. *Am J Clin Pathol* 1954;**24**: 1324–1328.
34. Wong MC, van Diepen JA, Hu L, Guigas B, de Boer HC, van Puijvelde GH, Kuiper J, van Zonneveld AJ, Shoelson SE, Voshol PJ, Romijn JA, Havekes LM, Tamsma JT, Rensen PCN, Hiemstra PS, Berbée JFP. Hepatocyte-specific IKKbeta expression aggravates atherosclerosis development in APOE*3-Leiden mice. *Atherosclerosis* 2012; **220**:362–368.
35. Zhang F, Hao GY, Shao ML, Nham K, An Y, Wang Q, Zhu Y, Kusminski CM, Hassan G, Gupta RK, Zhai QW, Sun XK, Scherer PE, Oz OK. An adipose tissue atlas: an image-guided identification of human-like BAT and beige depots in rodents. *Cell Metab* 2018;**27**:252–262 e253.
36. Woo CY, Jang JE, Lee SE, Koh EH, Lee KU. Mitochondrial dysfunction in adipocytes as a primary cause of adipose tissue inflammation. *Diabetes Metab J* 2019;**43**:247–256.
37. Lin Z, Tian H, Lam KS, Lin S, Hoo RC, Konishi M, Itoh N, Wang Y, Bornstein SR, Xu A, Li X. Adiponectin mediates the metabolic effects of FGF21 on glucose homeostasis and insulin sensitivity in mice. *Cell Metab* 2013;**17**:779–789.
38. Endo-Umeda K, Makishima M. Liver X receptors regulate cholesterol metabolism and immunity in hepatic nonparenchymal cells. *IJMS* 2019;**20**:5045.
39. Mindur JE, Swirski FK. Growth factors as immunotherapeutic targets in cardiovascular disease. *Arterioscler Thromb Vasc Biol* 2019;**39**:1275–1287.
40. Sonoda J, Chen MZ, Baruch A. FGF21-receptor agonists: an emerging therapeutic class for obesity-related diseases. *Horm Mol Biol Clin Investig* 2017;**30**: 20170002.
41. Fisher FM, Kleiner S, Douris N, Fox EC, Mepani RJ, Verdeguer F, Wu J, Kharitonenkov A, Flier JS, Maratos-Flier E, Spiegelman BM. FGF21 regulates PGC-1alpha and browning of white adipose tissues in adaptive thermogenesis. *Genes Dev* 2012;**26**:271–281.
42. Andersen B, Straarup EM, Heppner KM, Takahashi DL, Raffaele V, Dissen GA, Lewandowski K, Bodvarsdottir TB, Raun K, Grove KL, Kievit P. FGF21 decreases body weight without reducing food intake or bone mineral density in high-fat fed obese rhesus macaque monkeys. *Int J Obes (Lond)* 2018;**42**:1151–1160.
43. Bartelt A, Bruns OT, Reimer R, Hohenberg H, Ittrich H, Peldschus K, Kaul MG, Tromsdorf UI, Weller H, Waurisch C, Eychmuller A, Gordts PL, Rinninger F, Bruegelmann K, Freund B, Nielsen P, Merkel M, Heeren J. Brown adipose tissue activity controls triglyceride clearance. *Nat Med* 2011;**17**:200–205.
44. Khedoe PP, Hoeke G, Kooijman S, Dijk W, Buijs JT, Kersten S, Havekes LM, Hiemstra PS, Berbee JF, Boon MR, Rensen PC. Brown adipose tissue takes up plasma triglycerides mostly after lipolysis. *J Lipid Res* 2015;**56**:51–59.
45. Bakker LE, Boon MR, van der Linden RA, Arias-Bouda LP, van Klinken JB, Smit F, Verberne HJ, Jukema JW, Tamsma JT, Havekes LM, van Marken Lichtenbelt WD, Jazet IM, Rensen PC. Brown adipose tissue volume in healthy lean south Asian adults compared with white Caucasians: a prospective, case-controlled observational study. *Lancet Diabetes Endocrinol* 2014;**2**:210–217.
46. Kusminski CM, Scherer PE. Mitochondrial dysfunction in white adipose tissue. *Trends Endocrinol Metab* 2012;**23**:435–443.
47. Koh EH, Park JY, Park HS, Jeon MJ, Ryu JW, Kim M, Kim SY, Kim MS, Kim SW, Park IS, Youn JH, Lee KU. Essential role of mitochondrial function in adiponectin synthesis in adipocytes. *Diabetes* 2007;**56**:2973–2981.
48. Gaich G, Chien JY, Fu H, Glass LC, Deeg MA, Holland WL, Kharitonenkov A, Bumol T, Schilske HK, Moller DE. The effects of LY2405319, an FGF21 analog, in obese human subjects with type 2 diabetes. *Cell Metab* 2013;**18**:333–340.
49. Lee P, Linderman JD, Smith S, Brychta RJ, Wang J, Idelson C, Perron RM, Werner CD, Phan GQ, Kammula US, Kebebew E, Pacak K, Chen KY, Celi FS. Irisin and FGF21 are cold-induced endocrine activators of brown fat function in humans. *Cell Metab* 2014;**19**:302–309.
50. Owen BM, Ding XS, Morgan DA, Coate KC, Bookout AL, Rahmouni K, Kliewer SA, Mangelsdorf DJ. FGF21 acts centrally to induce sympathetic nerve activity, energy expenditure, and weight loss. *Cell Metab* 2014;**20**:670–677.
51. Ma W, Zhao D, He F, Tang L. The role of Kupffer cells as mediators of adipose tissue lipolysis. *J Immunol* 2019;**203**:2689–2700.
52. Goudriaan JR, Dahlmans VE, Teusink B, Ouwens DM, Febbraio M, Maassen JA, Romijn JA, Havekes LM, Voshol PJ. CD36 deficiency increases insulin sensitivity in muscle, but induces insulin resistance in the liver in mice. *J Lipid Res* 2003;**44**: 2270–2277.
53. Bao LC, Yin J, Gao W, Wang Q, Yao WB, Gao XD. A long-acting FGF21 alleviates hepatic steatosis and inflammation in a mouse model of non-alcoholic steatohepatitis partly through an FGF21-adiponectin-IL17A pathway. *Br J Pharmacol* 2018;**175**: 3379–3393.
54. Wang N, Li JY, Li S, Guo XC, Wu T, Wang WF, Li DS. Fibroblast growth factor 21 regulates foam cells formation and inflammatory response in Ox-LDL-induced THP-1 macrophages. *Biomed Pharmacother* 2018;**108**:1825–1834.
55. Borges MC, Lawlor DA, de Oliveira C, White J, Horta BL, Barros AJ. Role of adiponectin in coronary heart disease risk: a mendelian randomization study. *Circ Res* 2016; **119**:491–499.
56. Basurto L, Gregory MA, Hernández SB, Sánchez-Huerta L, Martínez AD, Manuel-Apolinar L, Avelar FJ, Alonso LAM, Sánchez-Arenas R. Monocyte chemoattractant protein-1 (MCP-1) and fibroblast growth factor-21 (FGF-21) as biomarkers of subclinical atherosclerosis in women. *Exp Gerontol* 2019;**124**:110624.

Translational perspectives

Current therapeutics does not fully block atherosclerosis development, indicating a need for additional effective therapeutics. Here, we demonstrate that pharmacological treatment with recombinant FGF21 potently protects against atherosclerosis in APOE*3-Leiden.CETP mice. Mechanistically, FGF21 reduces hypercholesterolaemia by accelerating triglyceride-rich lipoprotein turnover as a result of enhancing adipose tissue thermogenesis, thereby alleviating atherosclerotic lesion formation and severity. Consistent with our animal findings, FGF21 administration in obese patients has shown to reduce several cardiovascular risk factors such as obesity and dyslipidemia. Therefore, our present results, together with available clinical data, suggest that FGF21 is a promising therapeutic for atherosclerotic diseases.